Optimal oblique transition

ALESSANDRO BOTTARO[1]†, JAN. O. PRALITS[1] and STEFANIA CHERUBINI[2]

[1]DICCA, Università di Genova, Via Montallegro 1, 16145 Genova, Italy
[2]DMMM, Politecnico di Bari, Via Re David 200, 70126 Bari, Italy

(Received 26 May 2017)

A weakly nonlinear approach is described to identify the couple of oblique waves capable to optimally excite transition to turbulence in a plane shear flow. Optimal oblique wave pairs are found to exist in a very narrow wavenumber range – demonstrating the strong selectivity of the identified mechanism – and lead to rapid breakdown past a well defined threshold value of the disturbance amplitude. Direct numerical simulations of the Navier-Stokes equations corroborate the weakly nonlinear results.

1. Introduction

The breakdown of laminar shear flows is a central problem in fluid mechanics since the early experiments by Reynolds (1883*a*,*b*) in pipe flow. Despite the simplicity of unidirectional shear flows (plane Poiseuille and Hagen-Poiseuille, Couette, water-table flows and combinations thereof), the physical processes by which environmental effects trigger transition to turbulence are still largely unexplained; this is partly due to the fact that such flows undergo transition at Reynolds numbers for which the linear hydrodynamic stability equations predict a stable behavior, and to the non-normal nature of the equations themselves. The transition phenomenon in such flows must thus be based on nonlinear mechanisms, possibly exploiting transient disturbance energy amplification.

A recent approach to identify initial disturbances of finite amplitude capable to optimally initiate the transition process relies on nonlinear optimization theory. A complete review of the theory is given by Kerswell *et al.* (2014) and Luchini & Bottaro (2014). Such a theory is very powerful, the main drawback being that it is virtually impossible to explore the full parameter space, because of the computational cost of carrying out many direct simulations in the adjoint looping procedure until convergence of the chosen cost functional, for each set of parameters.

The need for an alternative optimization strategy is here coupled to the investigation of a physical mechanism believed to be central to turbulence breakdown in parallel shear flows: the growth and interaction of oblique waves.

In a recent paper, Pralits *et al.* (2015) have described a weakly non-linear approach capable to identify disturbances growing optimally on top of a mean flow distorted by the Reynolds stresses produced by the disturbances themselves. The results of that study depart significantly from previous, linear, optimal perturbation analyses and point to very receptive regions of wavespace which can support a self-sustaining cycle, as demonstrated by companion numerical simulations. That analysis was however truncated too early (in terms of the Fourier modes retained) to allow the determination of correct threshold amplitudes of transition to turbulence. The goal which we set in the present paper is to extend that work to identify the couple of obliquely travelling waves capable to optimally trigger transition.

† Email address for correspondence: alessandro.bottaro@unige.it

The role and importance of oblique waves in the breakdown of shear flow is by-now well established. The original work on the issue dates to the early nineties, when Schmid & Henningson (1992) described a transition scenario in plane Poiseuille flow which occurred on a much faster time scale than that based on the three-dimensional destabilization of initially two-dimensional streamwise travelling waves. Interestingly, the oblique transition scenario by Schmid & Henningson was sped up by an increase in initial amplitude and wave angle; waves with a spanwise wavenumber β larger than the streamwise one (α) experienced more rapid amplification and faster spreading of the spectral energy into modes with high streamwise wavenumbers.

Here, the oblique transition scenario is optimized by focussing on the oblique waves and on the ensuing streamwise streak/vortex mode; the initial (algebraic) growth of the oblique waves in subcritical conditions is enhanced by the presence of a strong mean flow distortion, in an interaction process which feeds onto itself. Somewhat suprisingly, the transition threshold of the weakly nonlinear approach is robust, i.e. it is confirmed by direct numerical simulations.

2. Formulation of the weakly non-linear problem

The decomposition of the whole field starts by considering a pair of oblique waves of wavevector $(\alpha, \pm\beta)$ and amplitude ϵ. First-generation interactions yield two ϵ^2 terms: one represents the mean flow correction, denoted with subscript 00, and the second, which behaves like $e^{2i\beta z}$, represents a streamwise-independent streak/vortex. Other first-generation terms of wavevectors $(2\alpha, 0)$ and $(2\alpha, \pm 2\beta)$ are not included on account of the numerical results by Schmid & Henningson (1992) which show that such terms are of smaller amplitude than the others. This aspect will be elaborated further on. The decomposition reads:

$$\begin{bmatrix} U(y) \\ 0 \\ 0 \\ P(x) \end{bmatrix} + \epsilon \begin{bmatrix} u_{1\pm1}(y,t) \\ v_{1\pm1}(y,t) \\ w_{1\pm1}(y,t) \\ p_{1\pm1}(y,t) \end{bmatrix} e^{i(\alpha x \pm \beta z)} + \epsilon^2 \begin{bmatrix} u_{00}(y,t) \\ v_{00}(y,t) \\ w_{00}(y,t) \\ p_{00}(y,t) \end{bmatrix} + \epsilon^2 \begin{bmatrix} u_{02}(y,t) \\ v_{02}(y,t) \\ w_{02}(y,t) \\ p_{02}(y,t) \end{bmatrix} e^{2i\beta z} + c.c., \quad (2.1)$$

with both the base flow $[U, 0, 0, P]^T$ and the mean flow distortion purely real fields; *c.c.* indicates the complex conjugate of a complex vector, also indicated with the superscript * next to the name of the variable. Replacing into the Navier-Stokes equations, collecting like-order terms and invoking the technique of *composite asymptotic approximations* (Cousteix & Mauss 2007), we find at order zero the (real) equation for the base flow:

$$\frac{\mathrm{d}P}{\mathrm{d}x} = \frac{1}{Re}\frac{\mathrm{d}^2U}{\mathrm{d}y^2}, \quad (2.2)$$

with Re the Reynolds number. In the Couette flow case considered here Re is based on the half-channel thickness, h, the modulus of the plates' velocity, $\mathcal{U}$, and the kinematic viscosity, ν; thus $\dfrac{\mathrm{d}P}{\mathrm{d}x} = 0$ and $U = y$, with y ranging from -1 to +1. At order ϵ, two

systems for modes (α,β) and $(\alpha,-\beta)$ are found. The system for mode (α,β) reads:

$$i\alpha u_{11} + v_{11y} + i\beta w_{11} = 0, \tag{2.3}$$

$$u_{11t} + i\alpha(U+\epsilon^2 u_{00})u_{11} + v_{11}(U+\epsilon^2 u_{00})_y + i\alpha p_{11} = \frac{1}{Re}\Delta u_{11}, \tag{2.4}$$

$$v_{11t} + i\alpha(U+\epsilon^2 u_{00})v_{11} + p_{11y} = \frac{1}{Re}\Delta v_{11}, \tag{2.5}$$

$$w_{11t} + i\alpha(U+\epsilon^2 u_{00})w_{11} + i\beta p_{11} = \frac{1}{Re}\Delta w_{11}, \tag{2.6}$$

where $\Delta = \partial^2/\partial y^2 - \alpha^2 - \beta^2$. In equations (2.3-2.6) subscripts t and y denote partial differentiation with respect to time and to the wall-normal coordinate. These equations are accompanied by no-slip conditions on both the upper and lower walls and by an initial condition $\mathbf{u}_{11}(y,t=0)$ which we will optimize for (the notation $\mathbf{u}_{ij} = (u_{ij}, v_{ij}, w_{ij})$ is used). The system of equations which yields $\mathbf{u}_{1-1}$ is the same as (2.3-2.6) except for replacing $+i\beta$ with $-i\beta$ everywhere, and symmetry yields $(u_{1-1}, v_{1-1}, w_{1-1}) = (u_{11}, v_{11}, -w_{11})$. At $\mathcal{O}(\epsilon^2)$ two further systems describing, respectively, the streamwise-independent modes (0,0) and (0,2β) are found. The first is the purely real system:

$$u_{00t} - \frac{1}{Re}u_{00yy} = F_u, \quad v_{00} = w_{00} = 0, \quad p_{00y} = F_v, \tag{2.7}$$

while the second is a complex system:

$$v_{02y} + 2i\beta w_{02} = 0, \tag{2.8}$$

$$u_{02t} + v_{02}(U+\epsilon^2 u_{00})_y - \frac{1}{Re}(u_{02yy} - 4\beta^2 u_{02}) = f_u, \tag{2.9}$$

$$v_{02t} + p_{02y} - \frac{1}{Re}(v_{02yy} - 4\beta^2 v_{02}) = f_v, \tag{2.10}$$

$$w_{02t} + v_{02}(\epsilon^2 w_{00})_y + 2i\beta p_{02} - \frac{1}{Re}(w_{02yy} - 4\beta^2 w_{02}) = f_w, \tag{2.11}$$

plus no-slip conditions at the walls for both set of modes. System (2.7) is ruled by a normal operator and growth is uniquely related to the terms on the right hand sides of the equations; conversely, the operator of the (0,2β) mode is nonnormal so that the mode is susceptible to large transient amplification. The streamwise-independent modes are forced in the momentum equations by the Reynolds stress vectors (F_u, F_v) and (f_u, f_v, f_w) which arise from primary interactions. All forcing terms are real, aside from f_w which is purely imaginary; they read:

$$F_u = -2v_{11}u^*_{11y} + 2i\beta w_{11}u^*_{11} - \epsilon^2(v_{02}u^*_{02y} - 2i\beta w_{02}u^*_{02}) + c.c.,$$
$$F_v = -2i\alpha u^*_{11}v_{11} - 2v_{11}v^*_{11y} + 2i\beta w_{11}v^*_{11} - \epsilon^2(v_{02}v^*_{02y} - 2i\beta w_{02}v^*_{02}) + c.c.,$$

and

$$f_u = -v_{11}u^*_{11y} - i\beta w_{11}u^*_{11} + c.c.,$$
$$f_v = i\alpha u_{11}v^*_{11} - v_{11}v^*_{11y} - i\beta w_{11}v^*_{11} + c.c.,$$
$$f_w = -i\alpha u_{11}w^*_{11} + v_{11}w^*_{11y} + i\beta w_{11}w^*_{11} - c.c.$$

The key point of the analysis is the fact of retaining the x-component of the velocity at $\mathcal{O}(\epsilon^2)$ in equations (2.4-2.6) to allow a distortion of the mean state above which oblique

waves, denoted by subscript 11, are superposed (note also that we have anticipated the fact that $v_{00} = w_{00} = 0$ in writing equations 2.4-2.6).

System (2.3–2.6) plus equations (2.7) and (2.8–2.11) are solved by maximizing the total energy of the unsteady perturbation

$$e(t) = e_{11}(t) + e_{1-1}(t) + e_{02}(t), \tag{2.12}$$

evaluated at a given final time $t = T$. The different contributions are defined by

$$e_{11}(t) = \frac{\epsilon^2}{2}\int_{-1}^{1} \mathbf{u}^*_{11}(y,t)\cdot\mathbf{u}_{11}(y,t)\,dy, \qquad e_{02}(t) = \frac{\epsilon^4}{2}\int_{-1}^{1} \mathbf{u}^*_{02}(y,t)\cdot\mathbf{u}_{02}(y,t)\,dy.$$

and $e_{1-1}(t) = e_{11}(t)$, by definition. The choice of the optimization functional is not unique, but it is expected that just about any objective functional which takes on heightened values at the target time T is suitable and leads to similar optimal solutions (Kerswell *et al.* 2014). This is also borne out by a comparison between the NLOP† in plane Couette flow of Monokrousos *et al.* (2011) (objective was the total viscous dissipation, integrated from $t = 0$ to $t = T$) and those by Rabin *et al.* (2012) (objective was the total kinetic energy at the final time, $t = T$).

For assigned ϵ the present weakly nonlinear problem is solved iteratively as follows:

(a) Maximise the energy $e(T)$, constrained by equations (2.3)-(2.6), over a given time span T, to find u_{11}, v_{11}, w_{11}. The optimization procedure is performed via adjoint looping; in the first iteration u_{00} is set equal to 0 $\forall y, t$.

(b) Compute the Reynolds stress components (f_u, f_v, f_w) and then solve the linear convection-diffusions equations (2.8–2.11) for the vortex/streak $\mathbf{u}_{02}$, with zero initial conditions for the velocity components.

(c) Evaluate the right hand side F_u of equation (2.7) for the u_{00} component, including the seemingly negligible terms of $\mathcal{O}(\epsilon^2)$, and solve for $u_{00}(y,t)$ under the initial condition $u_{00}(y,0) = 0$; equation (2.7) is a heat equation with the Reynolds stress term acting as source. Then, go back to (a).

(d) Stop the procedure when the relative difference in final wave energy, $e(T)$, is lower than 10^{-8}. The normalization employed is $e(0) = 2\epsilon^2$.

2.1. *Numerical procedures*

The problem outlined at step (a) in the solution procedure is a constrained maximization problem which can be solved using Lagrange multipliers. The governing equations are written in primitive variable form and the resulting adjoint equations are derived using a discrete approach (see Luchini & Bottaro 2014). The spatial derivatives are discretized using second order finite differences and a semi-implicit second-order scheme is used to advance in time. A uniform grid is used in the y-direction and 300 discrete points are sufficient to obtain a converged solution. The code has been tested on several cases found in the literature for $\epsilon \to 0$ (when the mean flow is not distorted); in particular, the value of the optimal gain $e_{11}(T)/e_{11}(0) = 0.00118\,Re^2$ and the corresponding time at which it is achieved, $T = 0.117\,Re$, with $\alpha = 35/Re$ and $\beta = 1.60$, are recovered to within 0.1% (Schmid & Henningson 2001).

Direct numerical simulations of the full nonlinear equations are also conducted, starting from the optimal initial conditions of the weakly nonlinear analysis, to confirm the weakly nonlinear results in the initial phases, before the amplification of harmonics which cannot be accounted for in the weakly nonlinear analysis. The code employed is the same used

† *Non Linear Optimal Perturbations*, as by the terminology introduced by Pringle & Kerswell (2010).

by Pralits *et al.* (2015); the computational domain has length $2\pi/\alpha$ along the streamwise direction and $2\pi/\beta$ along the span. The domain is discretized using a staggered grid and the Navier-Stokes equations are solved by a fractional-step method which is second-order accurate in space and time (Verzicco & Orlandi 1996). For each of the considered domains a different (uniform) discretization grid has been used, to keep the cell size approximately constant ($\Delta x \approx \Delta z \approx 0.1$, $\Delta y \approx 0.02$). A constant time step $\Delta t = 0.05$ has been chosen, ensuring the stability of the time discretization scheme ($CFL < 1$). The numerical convergence of the results has been checked by halving the cell size in the three space directions (and adjusting the time step consequently) and comparing the evolution of the energy in time.

3. Weakly non-linear results

The weakly nonlinear results for a representative case ($Re = 400$) are displayed in figure 1 for three values of ϵ and the final time fixed at $T = 80$. The choice of the time horizon T stems from the considerations which follow. First, for numerical convergence reasons, we want to ensure that the functional values attained at the final state are well separated from those of the laminar fixed point, and for this to occur the final time needs to be sufficiently large. Second, given that it takes some time to reach a (fully nonlinear) turbulent state starting from a slightly perturbed laminar flow, the choice of a short time horizon would produce initial conditions which optimize events such as transient bursts (Cherubini & De Palma 2013), not yielding states capable to self sustain for long times. This is also consistent with the known fact that the amplification of oblique waves occurs over a time scale which is intermediate between the short scale which characterizes the Orr-related amplification and the long time scale of the lift-up effect. Third, a recent study on (linear) localized optimal disturbances in a turbulent boundary layer, modelled by the Reynolds-Tiederman turbulent mean profile, shows that elongated streaks within the buffer layer of spanwise wavelength equal to about 100 wall units grow optimally over a time interval of about 80 viscous time units, for a large range of Reynolds numbers (Kim *et al.* 2016). Such a time scale is the eddy turnover time in the near-wall region of wall-bounded turbulent shear flows, and this result confirms that obtained earlier by Butler & Farrell (1992) on the mechanisms underlying the formation of turbulent streaks. Since $t^+ = t$ in the present Couette flow case, given that the friction velocity is simply $u_\tau = \sqrt{\nu \mathcal{U}/h}$, it is appropriate to take $T = 80$ as optimization interval. We have furthermore verified that setting another value of the target time in the interval $50 < T < 100$ does not yield substantial differences in the results.

Figure 1 summarizes the important results of the present study. When the disturbance amplitude is sufficiently low ($\epsilon < 0.00450$) the system behaves essentially in a linear fashion, with a peak in wave energy for $\alpha \to 0$ and $\beta = 1.54$. This initial condition has been called QLOP (*Quasi Linear Optimal Perturbation*) by Pringle & Kerswell (2010). Nevertheless, a second, very weak, energy peak ($2e_{11}(T)/e_{11}(0) \approx 20$) begins to emerge for $(\alpha, \beta) = (0.291, 1.039)$ (not visible in frame *a* of the figure because of the spacing chosen for the isolines). As ϵ increases (frame *b*) the energy gain associated to this second relative maximum becomes stronger, peaking at $(\alpha, \beta) = (0.27, 1.07)$. A further, very mild, increase in perturbation amplitude yields an explosive growth of the disturbance energy in a very narrow wavenumber range close to the second peak, with the appearance of a third energy peak. Frame *c* in figure 1 displays only a zoom of what goes on in the wavenumber neighborhood of the second and third peaks, the region around the first (quasi-linear) local maximum not showing any feature of note. The result to be highlighted is the strong selectivity of waves with (α, β) in a narrow range around

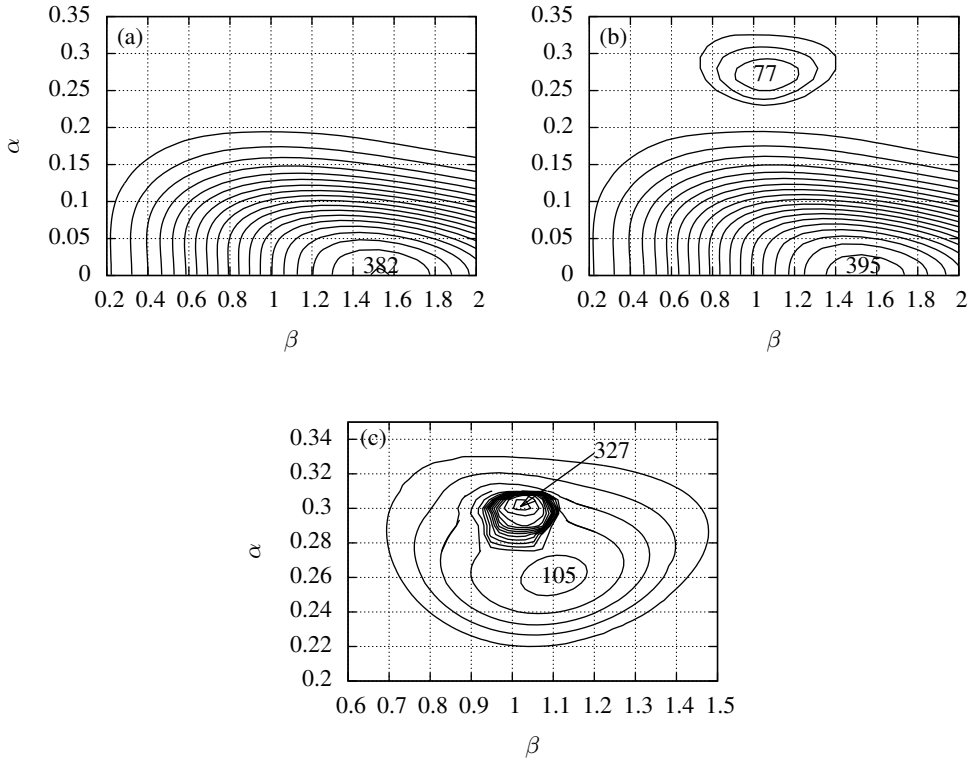

FIGURE 1. Iso-contours of the energy $2e_{11}(T)/e_{11}(0)$ in the $\alpha - \beta$ plane for the case of a) $\epsilon = 0.00450$ with maximum value equal to 382 at (α, β)=(0.001,1.540); b) $\epsilon = 0.00500$ with maximum value equal to 395 at (α, β)=(0.001,1.540) (the second peak in the frame has a maximum value of 77 at (α, β)=(0.270,1.070)); c) close-up around the second peak of frame b when $\epsilon = 0.00518$. A third peak with energy gain equal to 327 emerges at (α, β)=(0.303,1.020). The contour spacing is 20 in all frames.

$(0.303, 1.020)$; these numbers correspond to an optimal wave angle $\tan^{-1}(\beta/\alpha)$ of about 73^o, and this value is consistent with the conclusions reported by Schmid & Henningson (1992).

It is important at this point to analyse more in detail the disturbance wave energy as ϵ varies, shown in figure 2. The left frame demonstrates that the word "explosive" in defining the growth when ϵ exceeds 0.005 was not a misnomer, as the sudden rise of the red line in the figure clearly demonstrates, so that one can expect the triggering of a rapid transition to turbulence. The optimal wavenumbers for oblique transition are shown by red crosses in the right frame of the figure for the five cases computed with ϵ starting from 0.00518.

The significant conclusion is that a plane shear flow, such as Couette flow, is very receptive to oblique wave disturbances in a very narrow wavenumber range. Such disturbances have a well defined amplitude threshold above which large amplification takes place and are thus believed to facilitate the triggering of transition to turbulence. Direct Numerical Simulations (DNS) will next sustantiate these statements.

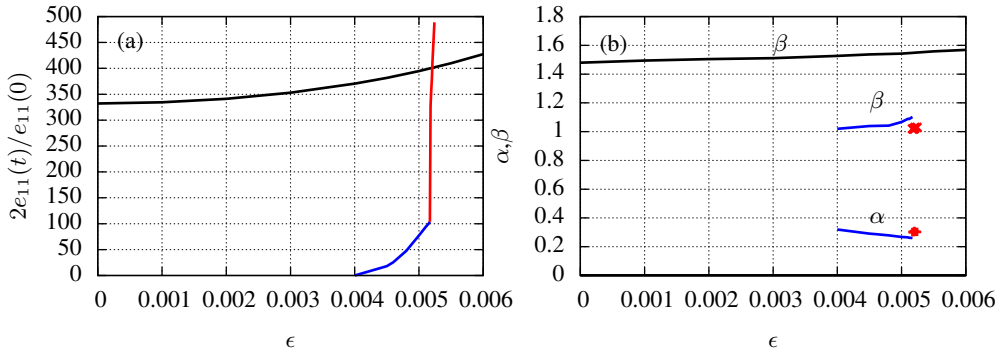

FIGURE 2. Values of a) the energy $2e_{11}(T)/e_{11}(0)$, and b) the corresponding wave numbers, at three different peaks as a function of ϵ. The black line corresponds to the case $\alpha \approx 0$ (for numerical reasons α cannot be set identically equal to zero, the value $\alpha = 0.001$ has thus been used to focus on quasi-streamwise-independent flow structures). The blue and red lines (and the markers) correspond to a second and third peak, respectively.

4. DNS results

Figure 3 shows a comparison between DNS and weakly nonlinear results for two different initial amplitudes, $\epsilon = 0.00450$ and $\epsilon = 0.00518$. For the smaller value of the amplitude the initial optimal solution is chosen to lie on the second energy peak (blue lines of figure 2), since an optimal solution on the first energy peak will lead to a direct relaminarization of the flow. For the larger amplitude case we have chosen to initiate the DNS from the optimal solution on the third energy peak. In particular, we select $(\alpha, \beta) = (0.291, 1.039)$ for $\epsilon = 0.00450$ and $(\alpha, \beta) = (0.303, 1.020)$ for $\epsilon = 0.00518$. For the two amplitudes, the initial growth of the weakly nonlinear model is very similar: in both cases the energy curve displays an inflection point at $t \approx 45$ followed by a relative maximum of the energy at $t \approx 70$. The local maximum of the disturbance energy $e(t)$ when $\epsilon = 0.00518$ is over twice as large that corresponding to an initial amplitude of 0.00450. The nonlinear simulations, for the same initial conditions, follow closely the weakly nonlinear curves up to $t \approx 20$ and depart from them when higher harmonics (displayed in figure 3, bottom frame) acquire importance. At $t = 20$ the flow structures which are set up by the weakly nonlinear model approach closely those which emerge from the fully nonlinear simulations. The subsequent evolution of the flow is that which one could forecast on the basis of the weakly nonlinear model, i.e. the lower amplitude flow remains for a while in the proximity of unstable saddles before escaping along the stable manifold towards the laminar fixed point. As the amplitude exceeds the $\epsilon = 0.00518$ threshold, the flow's trajectory remains chaotic for a long time (this has been verified running the DNS up to $t = 1000$). We cannot exclude that, for even longer times, the trajectory of this latter case could relaminarize, an event which can in principle be postponed "indefinitely" by choosing a computational box sufficiently large.

The energy content of individual Fourier modes is displayed in figure 3 (bottom frame) for $\epsilon = 0.00518$ for the first 100 units of time. The only modes which enjoy an appreciable growth in the time window examined are those displayed: the couple of oblique waves $(\alpha, \pm\beta)$ excites primarily modes $(0, 0)$ and $(0, 2\beta)$. The two-dimensional streamwise travelling wave $(2\alpha, 0)$ also grows rapidly initially but, for $t > 40$ remains consistently below the two main streamwise invariant modes. Whereas mode $(2\alpha, 0)$ could have been easily included in the weakly nonlinear model, its effect is not major and the modes included in the decomposition (2.1) are sufficient to represent the shape of the optimal oblique

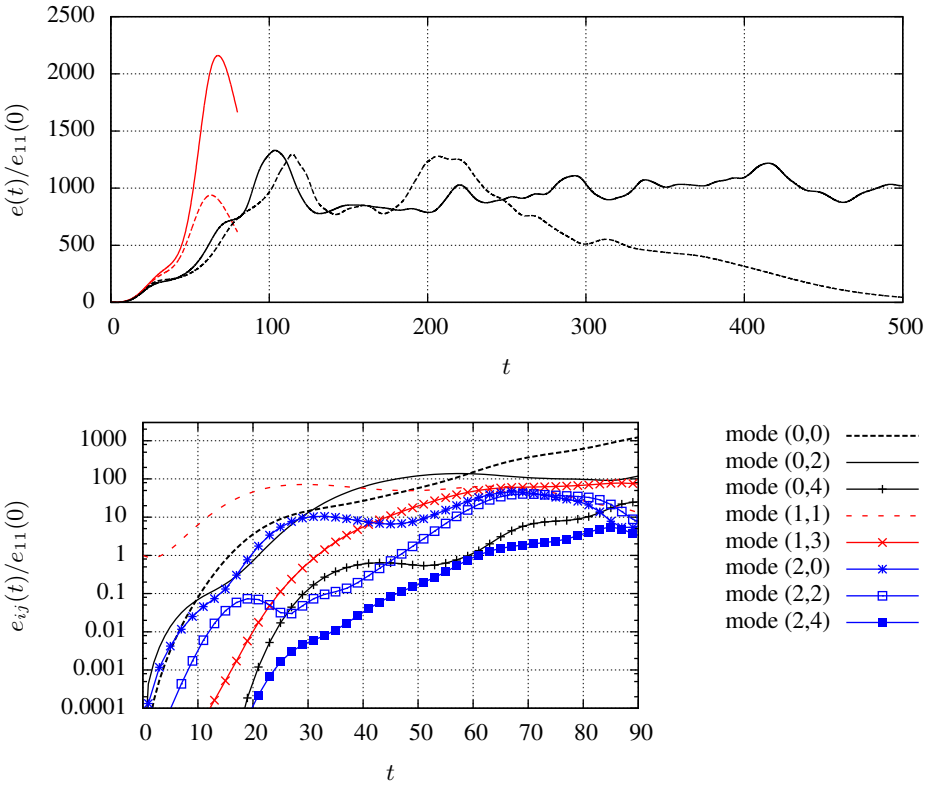

FIGURE 3. Top frame: $e(t)/e_{11}(0)$ for $\epsilon = 0.00450$ $(--)$ and $\epsilon = 0.00518$ $(-)$. Weakly nonlinear results (red lines) stop at $t = 80$. Bottom frame: $e_{ij}(t)/e_{11}(0)$ of different modes obtained from the DNS when $\epsilon = 0.00518$.

waves. We should stress once more that the key point of the whole weakly nonlinear analysis is the fact of having studied the growth of oblique waves sitting on top of a mean flow distorted by the $(0, 0)$ mode. It is clear that the long time behavior of the flow cannot be captured by the truncated model. Snapshots of such a behavior for supercritical conditions are presented in figures 4. The figure must be looked at as a cartoon, accompanying movies are also provided to enhance understanding. It is significant that the *minimal seed*† identified by Cherubini *et al.* (2011, 2012) via nonlinear optimizations re-appears also in the present case from primary waves interactions. It can be observed in figure 4 at $t = 40$; a similar flow structure is present also when $\epsilon = 0.00450$ but it is not of sufficient amplitude to trigger transition. This supports the hypothesis that the minimal seed is the smallest building block of transition to turbulence in parallel and quasi-parallel shear flows: the minimal seed evolves initially through tilting and amplification (Orr mechanism), and later through nonlinear interactions which lie at the heart of the turbulence regeneration cycle (cf., in particular, figure 4 of Cherubini *et al.* (2012)).

† The *minimal seed* is here defined as that coherent flow structure which is observed in the initial phases of transition. It is *recurrent* in that the same topology – albeit conveniently resized – is observed in different phases of the transition process. Conversely, Kerswell *et al.* (2014) use the definition of minimal seed to denote that destabilizing disturbance of smallest energy which sits near the laminar-turbulent boundary.

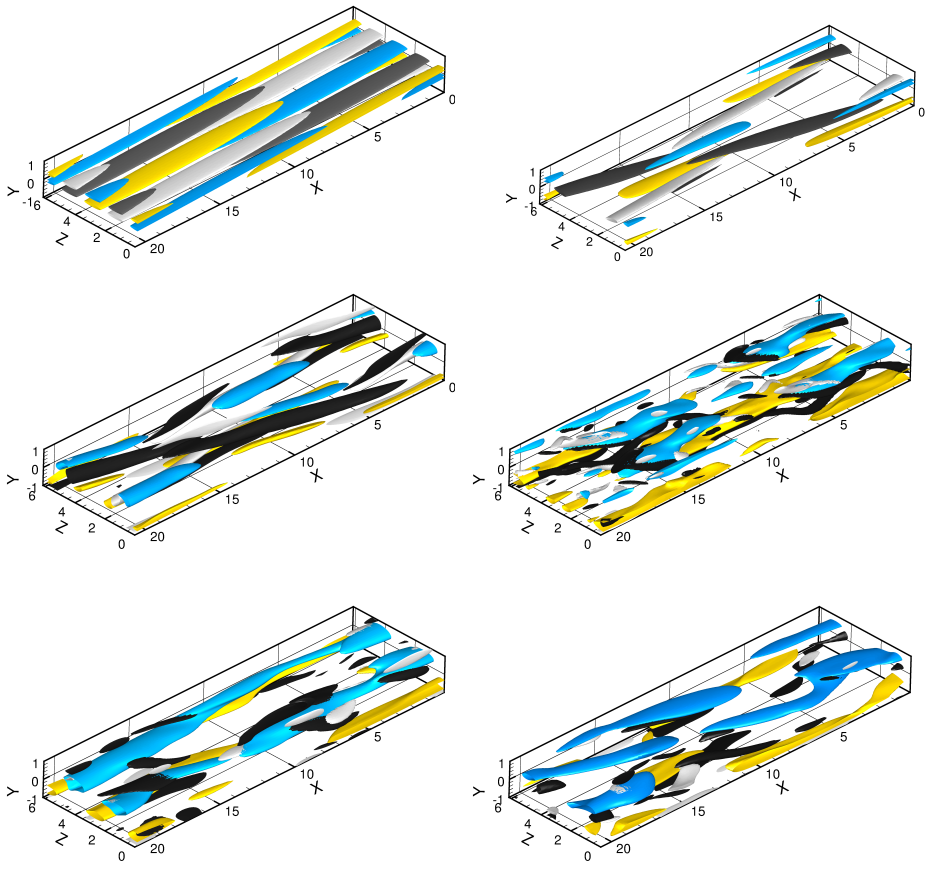

FIGURE 4. Streamwise velocity (positive blue, negative yellow) and streamwise vorticity (positive black, negative white) for the case in which $\epsilon = 0.00518$ and six different times (0, 40, 80, 120, 200, 300). Top left is $t = 0$ and bottom right is $t = 300$. The top right frame ($t = 40$) displays the typical shape of the *minimal seed* for Couette flow. The corresponding movie is available online, together with a movie for the case $\epsilon = 0.00450$ which relaminarizes.

5. Conclusions

A weakly nonlinear model has been developed to capture the couple of oppositely propagating waves capable to optimally induce transition in a simple shear flow; the model, which is simple and computationally inexpensive, contains the essential ingredients of the so-called oblique transition scenario. It is found that a $(\alpha, \pm\beta)$ wavenumber pair exists for which a very large growth of the perturbation energy ensues over a given time span. Such optimal wavevectors are very confined in wavespace and thus highly selective; they correspond to a wave angle of 73°. Whereas a monochromatic initial condition which deviates, even mildly, from the optimal wave pair would result in limited disturbance growth, initial conditions characterised by a white spectrum of wavelengths would inevitably filter the perturbation and yield, at large enough time, a signal with a strong mean flow distortion. The key of the whole weakly nonlinear approach is precisely that of considering perturbations which overlap onto a distorted mean flow. The surprising result is that a very large growth of the disturbance energy is suddenly found past a threshold amplitude of the initial oblique waves; this very same threshold is found to

separate a flow which relaminarizes from one which sustains turbulence in full numerical simulations initiated from the optimal oblique waves. The DNS further show that transition is mediated by a flow structure which has been christened the *minimal seed* by Cherubini *et al.* (2011, 2012), and which was earlier identified through (very costly) fully nonlinear optimizations. The weakly nonlinear model described here constitutes a convenient reduced-order model for a complete parametric inquiry of oblique transition in shear flows, allowing to select the few cases which might deserve additional insight through direct numerical simulations.

REFERENCES

Butler, K.M. & Farrell, B.F. 1992 Three-dimensional optimal perturbations in viscous shear flow. *Physics of Fluids* **4** (8), 1637–1650.

Cherubini, S. & De Palma, P. 2013 Nonlinear optimal perturbations in a Couette flow: bursting and transition. *J. Fluid Mech.* **716**, 251–279.

Cherubini, S., De Palma, P., Robinet, J.-C. & Bottaro, A. 2011 The minimal seed of turbulent transition in the boundary layer. *Journal of Fluid Mechanics* **689**, 221–253.

Cherubini, S., De Palma, P., Robinet, J-Ch. & Bottaro, A. 2012 A purely nonlinear route to transition approaching the edge of chaos in a boundary layer. *Fluid Dynamics Research* **44** (3), 031404.

Cousteix, J. & Mauss, J. 2007 *Asymptotic Analysis and Boundary Layers*. Springer-Verlag, Berlin.

Kerswell, R.R., Pringle, C.C.T. & Willis, A.P. 2014 An optimisation approach for analysing nonlinear stability with transition to turbulence in fluids as an exemplar. *Rep. Prog. Phys.* **77**, 085901.

Kim, E., Choi, H. & Kim, J. 2016 Optimal disturbances in the near-wall region of turbulent channel flows. *Phys. Rev. Fluids* **1**, 074403.

Luchini, P. & Bottaro, A. 2014 Adjoint equations in stability analysis. *Annual Review of Fluid Mechanics* **46** (1), 493–517.

Monokrousos, A., Bottaro, A., Brandt, L., Di Vita, A. & Henningson, D.S. 2011 Nonequilibrium thermodynamics and the optimal path to turbulence in shear flows. *Phys. Rev. Lett.* **106**, 134502.

Pralits, J. O., Bottaro, A. & Cherubini, S. 2015 Weakly nonlinear optimal perturbations. *J. Fluid Mech.* **785**, 135–151.

Pringle, C.C.T. & Kerswell, R.R. 2010 Using nonlinear transient growth to construct the minimal seed for shear flow turbulence. *Phys. Rev. Lett.* **105**, 154502.

Rabin, S.M., Caulfield, C.P. & Kerswell, R.R. 2012 Variational identification of minimal seeds to trigger transition in plane couette flow. *J. Fluid Mech.* **712**, 244–272.

Reynolds, O. 1883*a* An experimental investigation of the circumstances which determine whether the motion of water shall be direct or sinuous and of the law of resistance in parallel channels. *Proc. R. Soc. Lond. A.* **35**, 84–99.

Reynolds, O. 1883*b* An experimental investigation of the circumstances which determine whether the motion of water shall be direct or sinuous and of the law of resistance in parallel channels. *Phil. Trans. R. Soc. A* pp. 935–982.

Schmid, P.J. & Henningson, D.S. 1992 A new mechanism for rapid transition involving a pair of oblique waves. *Physics of Fluids A* **4** (9), 1986–1989.

Schmid, P.J. & Henningson, D.S. 2001 *Stability and Transition in Shear Flows. Applied Mathematical Sciences* v. 142. Springer New York.

Verzicco, R. & Orlandi, P. 1996 A finite-difference scheme for three-dimensional incompressible flows in cylindrical coordinates. *Journal of Computational Physics* **123** (2), 402 – 414.